Supporting information

Large-scale maritime transport of hydrogen: economic comparison of liquid hydrogen and methanol

Vladimir L. Meca[*1, a]*, Rafael d'Amore-Domenech* [a]*, Antonio Crucelaegui* [a]*, Teresa J. Leo* [a]

[a]Dept. Arquitectura, Construcción y Sistemas Oceánicos y Navales, ETSI Navales, Universidad Politécnica de Madrid, Avenida de la Memoria 4, Madrid 28040, Spain

Corresponding author:

[*]vl.meca@upm.es

[1]Permanent address: Dept. Arquitectura, Construcción y Sistemas Oceánicos y Navales, ETSI Navales, Universidad Politécnica de Madrid, Avenida de la Memoria 4, Madrid 28040, Spain

Number of pages: 35

Number of tables: 12

Number of figures: 4

Contents

1. Definition of alternatives

This study compares different options for the sea transport of hydrogen obtained by means of electrical energy from renewable sources. The alternatives analysed in this study are presented in Figures 1-3. The first, alternative A (Figure 1), is based on the generation of hydrogen from electrical energy of renewable origin; the transport of liquefied hydrogen and its regasification. The second, alternative B (Figure 2), is based on the generation of hydrogen from electrical energy of renewable origin; a subsequent synthesis process to use methanol as a hydrogen vector; methanol transport and finally a methanol-reforming process for obtaining hydrogen at destination. The third, alternative C (Figure 3), has the same scheme as the previous one, but instead of reforming, an electrolysis process is carried out to obtain hydrogen.

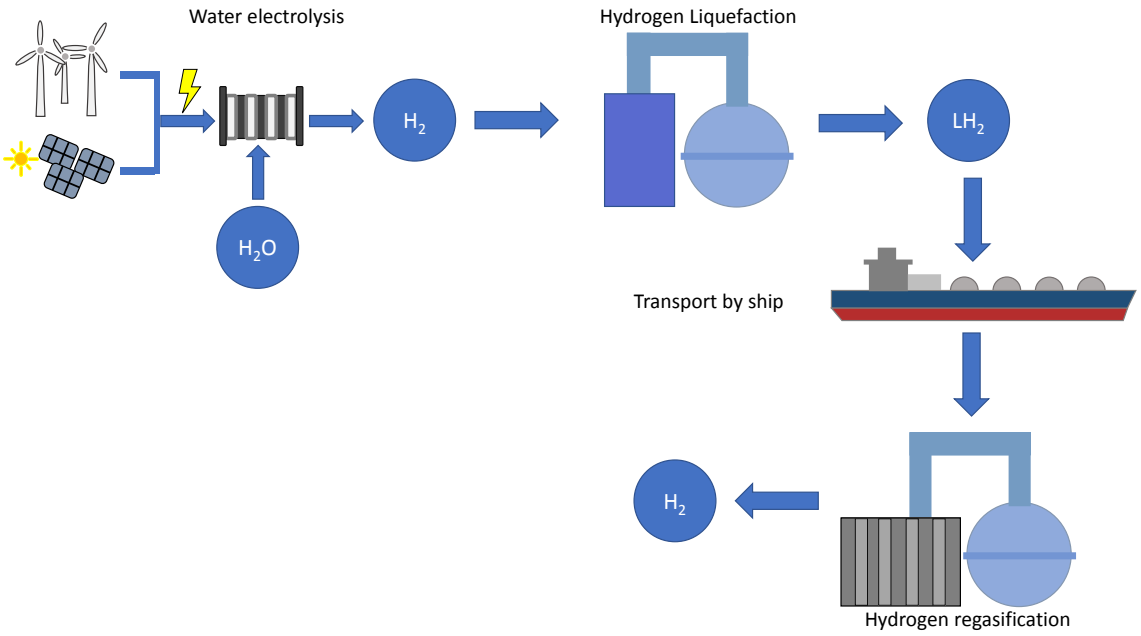

Figure S1. Alternative A. Liquefied hydrogen and its regasification.

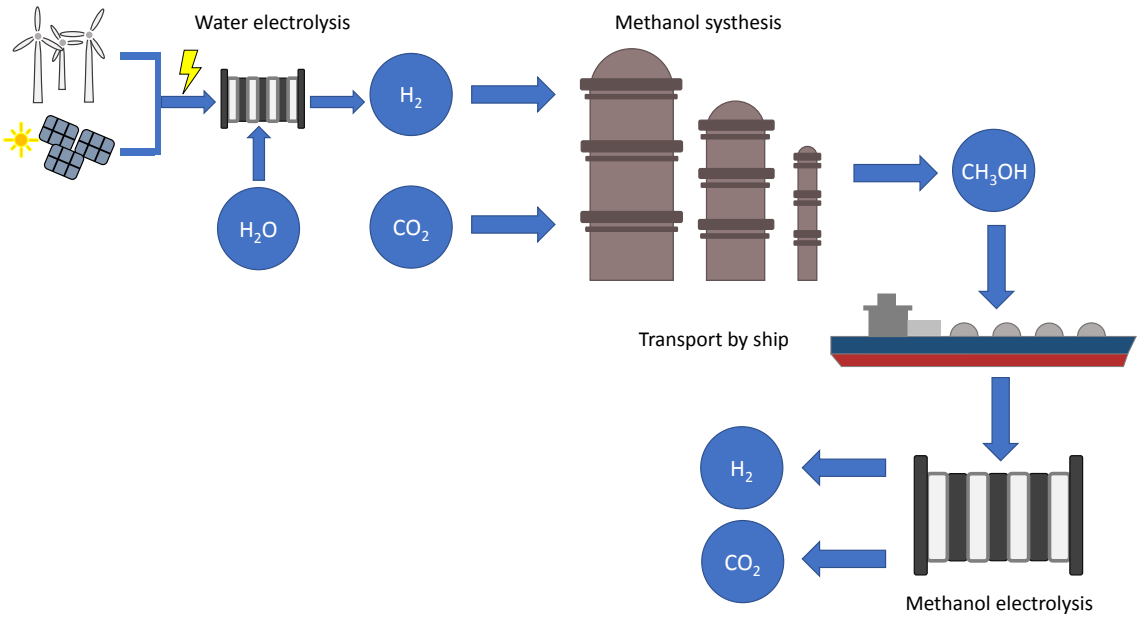

Figure S2. Alternative B. E-methanol to hydrogen through electrolysis.

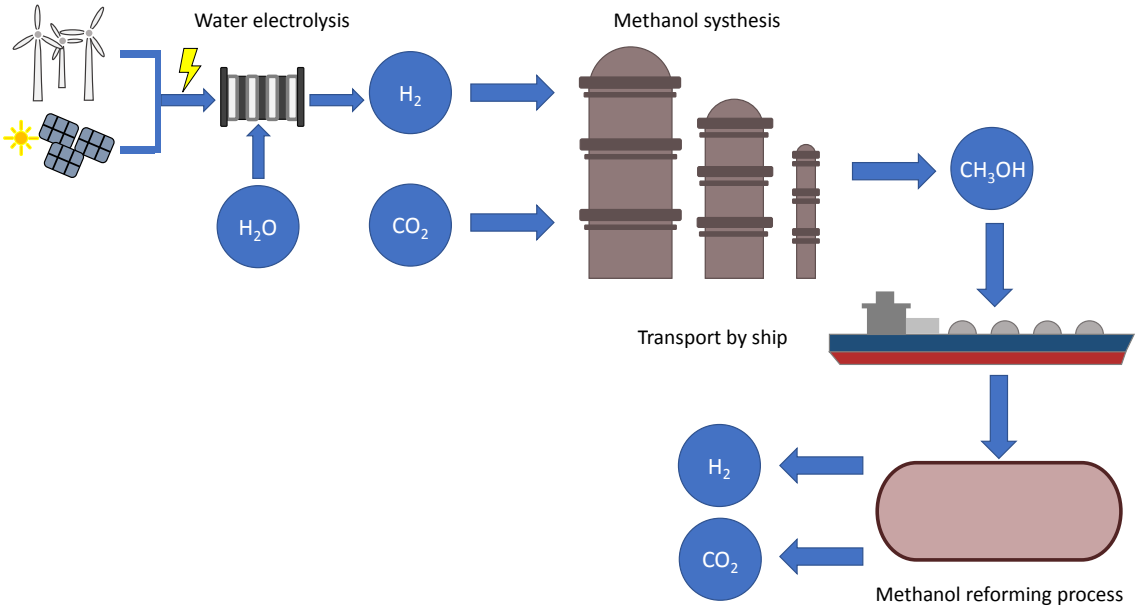

Figure S3. Alternative C. E-methanol to hydrogen by steam reforming.

Table S1 presents a summary of the components of the different alternatives and indicates which alternatives are involved in each of the facilities.

Table S1. Summary of the facilities that are part of the different alternatives studied.

	Water treatment plant	Water Electrolysis plant	Methanol synthesis plant	Hydrogen liquefaction plant	Methanol storage facilities (Export)	Liquid hydrogen storage facilities (Export)	Methanol carrier ship	LH2 carrier ship	Methanol storage facilities (Import)	Liquid hydrogen storage facilities (Export)	Methanol electrolysis plant	Steam reforming plant	Hydrogen regasification plant
Alternative A	x	x		x		x		x		x			x
Alternative B	x	x	x		x		x		x		x		
Alternative C	x	x	x		x		x		x			x	

2. Definition of models

In order to make consistent comparisons among all alternatives, a series of harmonisation assumptions have been made, which could be adjusted. The following are those established by the authors:

- All alternatives have a lifespan of 30 years.
- All the costs are calculated in 2021 USD.
- Regarding conversion from other currencies, conversion rates of the source year are used and then corrected for inflation.
- For this study, the annual inflation rate is assumed to have a constant value of 2.5%, which corresponds with average world inflation.[1]
- All the alternatives are subject to the following cost breakdown:
    - Infrastructure cost: that which is directly related to the creation of the infrastructure of the power link.
    - Operation and maintenance (O&M) cost: that which is related to the operation and maintenance of the infrastructure. This excludes the monetary cost of energy

losses and extraordinary interventions. Most references estimate the annual O&M cost as a percentage of total investment.[2]

- Mid-life (M-L) refurbishment cost: normally, mid-life refurbishments are completed in a single or multiple stages during the life of the power links. They are mostly conducted to update outdated systems or to replace those with a shorter lifespan than the complete infrastructure.
- End-of-life: at the end-of-life of the link, the existing obsolete installations will likely have to be de-commissioned and retired. Such de-commissioning has an associated cost. Other end-of-life strategies are also possible, however, they are not considered in this method in order to keep the analysis as simple as possible.
- Cost of energy losses: life-cycle energy losses of the link converted into monetary terms. They depend on the price of the electricity at the exportation end. The authors suggest exploring 100 USD/MWh (27.8 USD/GJ), 150 USD/MWh (41.7 USD/GJ) and 200 USD/MWh (55.6 USD/GJ).

- Regarding thermodynamic properties used for the energy loss estimation, all the thermodynamic properties are calculated using REFPROP[3] and the thermochemical data are extracted therefrom.[4]

2.1 Facilities shared between hydrogen and methanol alternatives

2.1.1 Water treatment plant

The cost models of the reverse osmosis plant for obtaining fresh water from seawater are obtained using information from El-Emam et al.[5] The system consists of two saltwater pumps, a filter, chemical treatment system, valve, RO reverse osmosis cartridges, Pelton turbine, and a mixing chamber. The low-pressure pump moves seawater to the filter. After the filter, the chemical treatment is applied to the water, or it is conducted through the valve to the end of the circuit, thereby creating a bypass. The chemically-treated water is moved to a high-pressure pump and subsequently, to an RO system. The brine water is taken to the Pelton turbine, and the treated water is mixed with the seawater from the bypass. From this mixture, the desired water is obtained.

Seawater intake and pre-treatment section (SWIP) includes a low-pressure pump, filter, and chemical treatment. Its purchased equipment cost is estimated using a correlation presented in El-Emam et al.[5] It has been modified to take annual inflation into account:

$$PC_{SWIP} = 1184 \cdot \dot{V}_t^{4/5} \quad \text{(Eq. S1)}$$

where $\dot{V}_t$ is the total fed seawater volume flow rate in m^3/day.

The annual cost of the energy consumed by the low-pressure pump is estimated in this study by the equation:

$$\dot{c}_{e,SWIP} = p_{SWIP} \cdot \dot{V}_t \cdot f_1 \cdot C_e / \eta_{SWIP} \quad \text{(Eq. S2)}$$

where P_{SWIP} is the pressure after the pump in kPa; $\dot{V}_t$ is the total fed seawater volume flow rate in m^3/s; f_1 is the plant load factor; C_e is the price of the electricity at the origin in \$/kWyear and η_{SWIP} is the low-pressure pump efficiency.

The purchase equipment cost of the high-pressure pump is estimated using the equation presented in El-Emam et al.[5] and modified to take into account annual inflation:

$$\log_{10}\left(\frac{PC_{HPP}}{1.189}\right) = 3.3892 + 0.0536\log_{10}(p_{HPP} \cdot \dot{V}_{RO} \cdot f_1 / \eta_{HPP}) + 0.1538\left[\log_{10}(p_{HPP} \cdot \dot{V}_{RO} \cdot f_1 / \eta_{HPP})\right]^2 \quad \text{(Eq. S3)}$$

where P_{HPP} is the pressure after the high-pressure pump in kPa; $\dot{V}_{RO}$ is the water volume flow rate of the pump in m^3/s and η_{HPP} is the high-pressure pump efficiency.

The annual cost of the energy consumed by the high-pressure pump is estimated using the same method as that presented for the low-pressure pump: replacing values of pressure and water volume flow rate after the high-pressure pump and its efficiency (90%).

RO membranes cost is calculated by the equation:

$$PC_{RO} = 10 \cdot N \cdot A \quad \text{(Eq. S4)}$$

where N is the number of membranes installed, and A is the area of each membrane.

The Pelton turbine purchase cost is calculated by the equation presented in El-Emam et al.[5] It has been adjusted for annual inflation:

$$\log_{10}\left(\frac{PC_{PT}}{1.189}\right) = 2.2476 + 1.4965\log_{10}(p_{PT} \cdot \dot{V}_{brine} \cdot f_1 \cdot \eta_{PT}) - 0.1618[\log_{10}(p_{PT} \cdot \dot{V}_{brine} \cdot f_1 \cdot$$

]^2 (Eq. S5)

where P_{PT} is the pressure before the turbine in kPa; $\dot{V}_{brine}$ is the brine volume flow rate of the turbine in m^3/s and η_{PT} is the turbine efficiency.

The O&M cost for the low-pressure pump, high-pressure pump, RO cartridges and turbine are defined as 5%, 4%, 1%, and 4% of the total capital investment (TCI), respectively. In this study, TCI is estimated as 6.32 times the equipment purchase cost.[6]

The annual cost of chemical treatment is defined as:[5]

$$\dot{c}_{op,ch} = \dot{V}_t \cdot f_1 \cdot C_{ch} \quad \text{(Eq. S6)}$$

where $\dot{V}_t$ is the total fed seawater volume flow rate in m^3/year, and C_{ch} is the cost of chemical treatment per water volume, 0.018 \$/m^3.

Two replacements of the low-pressure pump, high-pressure pump and turbine are foreseen during the life of the plant. Annual replacement cost of RO cartridges is calculated by:

$$\dot{c}_{op,RO} = r_m \cdot cc_{RO} \cdot \dot{V}_{RO} \quad \text{(Eq. S7)}$$

where r_m is the membrane replacement factor, 0.01; cc_{RO} is the cartridge filter cost, 0.01 \$/m^3 and $\dot{V}_{RO}$ is the water volume flow rate of the membranes in m^3/year.

Table S2 contains the baseline assumptions used for the thermo-economic calculations of the water treatment plant.

Table S2. Assumptions for the water treatment plant.

Parameter	Value	Uncertainty
η_{HPP} [5]	90%	5%
η_{SWIP} [5]	87%	5%
η_{PT} [5]	79%	5%
f_1	0.9	5%
r_m [5]	0.1	10%
C_{ch} (\$/m^3)[5]	0.018	5%

p_{SWIP} (kPa)[5]	650	5%
p_{HPP} (kPa)	5350	5%
p_{PT} (kPa)	5100	5%
cc_{RO} ($/m^3)[5]	0.01	5%
End of Life (%TCI)	10%	5%

2.1.2 Water electrolysis plant

In the cost breakdown of the entire hydrogen link, the electrolysis plant is one of the most important components. Therefore, the cost model should be as accurate as possible. Linear models are discarded since they do not consider the effects of scale of larger installations. For this reason, the investment cost must, at least, consider the effects of scale of the output hydrogen and the nominal efficiency of the plant. Under the designated efficiency, the electrolyser is to work under a specific current density. In this regard, the empirical equation defined for cost estimation of a PEM electrolysis plant, $C_{EC,}$ used by Lümmen et al.,[7] based on a previous one defined by Oi et al.,[8] is suitable for this work. Such equation, updated to 2021 monetary terms, expressed by the nominal mass flow rate of hydrogen is:

$$C_{EC} = 90588585 \cdot \frac{\dot{m}_{H_2}{}^{0.79}}{j^{0.32}} \quad \text{(Eq. S8)}$$

where $\dot{m}_{H_2}$ is expressed in (kg/s) and the current density j in ($\mathrm{A/cm^2}$).

The expected annual O&M cost is 1.5% of the installed cost.[9] The lifespan of an electrolyser may reach 100,000 h.[9] Therefore, at least two complete midlife refurbishments are foreseen.

The electric power consumed by the electrolysis plant $\dot{W}_{ext,electrol}$ can be calculated by:

$$\dot{W}_{ext,electrol} = \frac{\dot{m}_{\mathrm{H_2}} \cdot h_{\mathrm{H_2}} + \dot{m}_{\mathrm{O_2}} \cdot h_{\mathrm{O_2}} - \dot{m}_{\mathrm{H_2O}} \cdot h_{\mathrm{H_2O}}}{\eta_{electrol}} \quad \text{(Eq. S9)}$$

where $\dot{m}_{\mathrm{H_2}} = M_{\mathrm{H_2}}/M_{\mathrm{H_2O}} \cdot \dot{m}_{\mathrm{H_2O}}$; $\dot{m}_{\mathrm{O_2}} = M_{\mathrm{O_2}}/M_{\mathrm{H_2O}} \cdot \dot{m}_{\mathrm{H_2O}}/2$, and the enthalpies are obtained as:

$$h_{\mathrm{H_2}} = \Delta h^0_{f_{\mathrm{H_2}}} + \left[h_{\mathrm{H_2}}(T,p) - h_{\mathrm{H_2}}(T^0,p^0)\right] \quad \text{(Eq. S10)}$$

$$h_{\mathrm{O_2}} = \Delta h^0_{f_{\mathrm{O_2}}} + \left[h_{\mathrm{O_2}}(T,p) - h_{\mathrm{O_2}}(T^0,p^0)\right] \quad \text{(Eq. S11)}$$

$$h_{\mathrm{H_2O}} = \Delta h^0_{f_{\mathrm{H_2O}}} + \left[h_{\mathrm{H_2O}}(T,p) - h_{\mathrm{H_2O}}(T^0,p^0)\right] \quad \text{(Eq. S12)}$$

Thus, $\Delta h^0_{f_i}(T^0,p^0)$ is the enthalpy of formation of the substance i at (T^0,p^0), and $\left[h_{\mathrm{i}}(T,p) - h_i(T^0,p^0)\right]$ is the enthalpy increment of the substance i from (T^0,p^0) to (T,p).

The power consumed by the electrolysis plant does not coincide with the energy loss. This is because the electric energy in the electrolyser is being transformed into chemical energy by a form of hydrogen. If this transformation were reversible, the electrical power used would be $\dot{W}_{ext,electrol} = \dot{m}_{\mathrm{H_2}} \cdot HHV_{\mathrm{H_2}}$, where $HHV_{\mathrm{H_2}}$ is the higher heating value of hydrogen. However, they

do not coincide because $\eta_{electrol} < 1$. The difference is the energy lost in the form of heat. Therefore, the energy lost in the transformation of electricity into hydrogen is calculated by:

$$\left.\frac{dE}{dt}\right|_{lost} = \dot{W}_{ext,electrol} - \dot{m}_{\mathrm{H_2}} \cdot HHV_{\mathrm{H_2}} \quad \text{(Eq. S13)}$$

For the calculation of the levelized cost of hydrogen, $\dot{W}_{ext,electrol}$ will be used. However, for the life cycle cost of the link, $\left.\frac{dE}{dt}\right|_{lost}$ will be used.

Table S3 contains the baseline assumptions used for the thermo-economic calculations of the electrolysis plant.

Table S3. Assumptions for the water electrolysis plant

Parameter	Value	Uncertainty
j (A/cm^2)	1	5%
$\eta_{electrol}$	0.8	5%
Yearly O&M (%$C_{electrol}$)	1.5%	5%
M-L refurbishment (% $C_{electrol}$)	200%	5%
End of Life (%$C_{electrol}$)	10%	5%
T^0 (˚C)	25	1%
$T_{\mathrm{O_2}}$ (˚C)	80	1%
$T_{\mathrm{H_2}}$ (˚C)	80	1%

T_{H_2O} (˚C)	25	1%
p^0 (kPa)	100	1%
p_{O_2} (kPa)	5,000 (pipeline) 3,000 (LH_2 & cH_2)	1%
p_{H_2} (kPa)	5,000 (pipeline) 3,000 (LH_2 & cH_2)	1%
p_{H_2O} (kPa)	5,000 (pipeline) 3,000 (LH_2 & cH_2)	1%
$\Delta h^0_{f_{H_2}}$ (kJ/mol) [4]	0	0%
$\Delta h^0_{f_{O_2}}$ (kJ/mol) [4]	0	0%
$\Delta h^0_{f_{H_2O}}$ (kJ/mol) [4]	-285.830	0%
HHV_{H_2} (MJ/kg) [10]	141.88	0%

1.1 Exclusive facilities of hydrogen alternative

1.1.1 Hydrogen liquefaction plant

Different cost prediction models have been found, based on H2A models.[11] Since the largest hydrogen liquefaction plant is 30 t/d (0.35 kg/s),[12] it has been recommended not to extrapolate above 200 t/d (2.31 kg/s)[13]. However, the IEA report on the future of hydrogen assumed a capacity of the liquefaction plant of 712 t/d (8.24 kg/s) with an estimated cost of 1400.[14] If the extrapolation for 712 t/d is attempted with the prediction model from Chen [13], the estimated cost

is around 669 MUSD, but if instead the prediction model from HDSAM [11] is used, 1427 MUSD is the result. Therefore, although it might present a certain degree of uncertainty, the cost prediction model from HDSAM [11] allows reasonably accurate extrapolations for high liquefaction rates. The infrastructure cost for the liquefaction plant, C_{LP}, in 2018 USD is estimated by:

$$C_{LP} = 258912589 \cdot \dot{m}_{H_2}^{0.8} \quad \text{(Eq. S14)}$$

With C_{LP} in USD and $\dot{m}_{H_2}$ in (kg/s).

Liquefaction plants are very reliable with an annual availability of 98.5%.[13] The total annual O&M cost, excluding electricity, is estimated at approximately 3% of the total installation cost.[11] Several mid-life refurbishments are foreseen, as compressors, turbines, and pumps of the liquefaction plant will need to be replaced. In this regard, 40% of the total capital cost is foreseen, based on the assumption that approximately 20% of the total cost of the plant is associated with turbines, compressors, and pumps, which are components subject to mechanical wear.

The transformation of hydrogen into a liquefied state is considered an energy loss, as energy recovery systems are not considered in this work. In this regard, the energy losses will be

calculated by multiplying the mass of the produced hydrogen in the life cycle of the plant by the specific work for hydrogen liquefaction w_{liquef}. Table S4 contains the baseline assumptions used for the thermo-economic calculations of the hydrogen liquefaction plant.

Table S4. Assumptions for the liquefaction plant

Parameter	Value	Uncertainty
Yearly O&M ($\%C_{LP}$)	3%	5%
M-L refurbishment ($\%C_{LP}$)	40%	5%
End of Life ($\%C_{LP}$)	10%	5%
w_{liquef} (kWh/kg)[15]	6.1	3%
w_{liquef} (MJ/kg)[15]	22.0	3%

1.1.2 Liquid hydrogen storage facilities

The most cost-effective form of storing large quantities of liquid hydrogen is in double-walled spherical tanks. In such tanks, the outer wall is normally made of light steel, while the inner wall is often made of austenitic stainless steel. The annular space between both walls is filled with perlite whilst the air is evacuated to prevent it from condensing on the cryogenic inner wall. Regarding the cost model, HDSAM Version 3.0 incorporates specific cost data for this type of tank: 4,000 m^3 (280 t) and 1,000 m^3 (70 t), with an uninstalled cost of 7.217 MUSD (2014) and

1.684 MUSD (2014), respectively.[11] The IEA report on the future of hydrogen also includes data for a tank with a capacity of 3190 t of hydrogen, which has a cost of 290 MUSD (2018).[14] Within information published by Chen [13], a model for predicting spherical tank costs as a function of their size was made. Such model relied on economic data of this type of tank, which was available at that time. However, a new regression is made with the cost of the tanks, cited C_{LHT} above, in order to have a more recent cost model. Such regression follows a potential model as it is the one that best coincides with the available data. The explanation of this can be found in Appendix C. The resulting equation, from applying the potential curve fit is:

$$C_{LHT} = 0.51464 \cdot m_{H_2}^{1.344} \quad \text{(Eq. S15)}$$

With C_{LHT} expressed in USD and m_{H_2} in kg.

The installed cost can be estimated with a factor of 1.3 over the uninstalled cost of the spherical tank.[13]

The total O&M cost is estimated at approximately 3% of the total installed cost of the tank.[11] No mid-life refurbishments are foreseen for the liquid hydrogen storage system. Estimated energy losses of the tank involve the re-liquefaction energy of the boil-off of the stored hydrogen.

Table S5 contains the baseline assumptions used for the thermo-economic calculations of the liquid hydrogen tanks.

Table S5. Summary of the baseline assumptions for the liquefied storage calculations

Parameter	Value	Uncertainty
Yearly O&M ($\%C_{LHT}$)	3%	5%
M-L refurbishment ($\%C_{LHT}$)	0%	5%
End of Life ($\%C_{LHT}$)	10%	10%
$w_{reliquef}$ (kWh/kg)[15]	6.1	3%
$w_{reliquef}$ (MJ/kg)[15]	22.0	3%
Daily boiloff (% average m_{H_2} stored)	0.1%	5%
Average m_{H_2} stored ($\%m_{H_2}$ capacity)	50%	0%
Number of tanks	3	0%
Capacity of each tank ($\%m_L$)	33.33%	0%

1.1.3 LH2 carrier ship

There are two approaches regarding the operation of a ship for bulk hydrogen transportation from a financial viewpoint: either own a ship and be responsible for everything related to its operation or hire a ship and hold the shipowner responsible for part of the expenses of its operation in exchange for a charter rate, see Figure 2. There are basically three types of charters: bareboat charter, time charter, and voyage charter.[16,17] A Bareboat charter is an arrangement for

hiring a vessel for a specific period of time in which the shipowner is not responsible for the administration or technical maintenance of the ship. Thus, the charterer attains possession and complete control over the ship and is responsible for all the operating expenses.[17] This includes crew, consumables, maintenance, insurance, and port costs. A voyage charter is another type of contracting arrangement in which the shipowner is responsible for all the costs related to the voyage of the ship, including all port charges, except for the loading and unloading of the cargo when the contract is performed under FIO terms (Free In and Out).[17] Time charter is another type of contracting for a specific period whereby the shipowner is responsible for all the fixed costs and the charterer is only liable for non-fixed costs, such as consumables, commissions and port charges.[17]

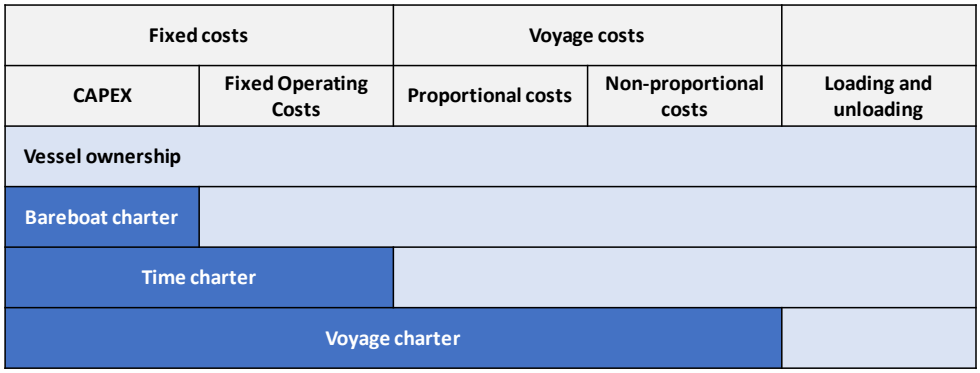

Figure S4. Options for the ship operation for bulk transportation of goods. The dark shaded items represent the costs that are covered by the shipowner, whereas the light shaded items represent the additional costs covered by the charterer.

For the intended form of ship operation, where a cargo ship will always have to travel between two points, the most desirable option would be a bareboat charter or time charter. This is because

owning a vessel immobilizes a great sum of capital and a voyage charter is often more expensive than the other two options. Between a bareboat charter and time charter, the second option is preferred by any company that is not specialized in shipping. This is because such companies normally do not benefit from the reduced operating costs as is the case with a specialized company. For these reasons, the most appropriate charter type for this context is the time charter, hence it is the one selected.

Time charter rates of bulk cargo ships source from different markets, according to the transported goods. Within those markets, the charter rate varies depending on a variety of factors: whether the chartering is for a spot or for long-term; the size of the ship and how modern the ship in question is. Very often, such markets are very transparent and competitive, thus, overall, the rates are supply-and-demand based, but the final rate is always negotiated on a case-by-case basis. The resulting freight rate depends on the bargaining power of shipowners and charterers.[17]

At present, there is no fleet in operation for bulk hydrogen transportation by ship, although in January of 2022 the Suiso Frontier from Kawasaki heavy industries started operating one.[18] Nevertheless, due to the similarities with the LNG, the LNG fleet can be used as a reference for

estimating LH_2 freight rates. This is applicable as well to the compressed natural gas (CNG) fleet for the cH_2 charter rate estimation.

Spot charter rates often refer to a contract term of six months or less.[19] In contrast, long-term charter rates refer to a contract term of more than 5 years.[19] The spot charter market is very volatile, whereas long-term charter rates are steadier.[17] For LNG, both spot and long-term charter rates follow a downward trend from the historic maximum reached in 2012, as a result of the Fukushima accident in 2011. The spot charter rates ranged from an average of 160 kUSD/d in the first quarter of 2012 to approximately 30 kUSD/d in mid-2015, which remained constant until mid-2017, when spot charter rates started to rise again. At the end of 2018, the average spot charter rate was 150 kUSD/d, but subsequently fell to 74 kUSD/d by January of 2019.[19] During this specific period, the long-term charter rates of LNG, started at approximately 90 kUSD/d in the first quarter of 2012, and steadily and slowly decreased until the first quarter of 2018 when they fell to 60 kUSD/d. At that point, the trend changed and it increased to approximately 70 kUSD/d for the last quarter of 2018.[19,20] Considering all the similarities, it is safe to assume a long-term time benchmark charter rate of 90 kUSD/d. for a hypothetical LH_2 of 180,000 m^3 Regarding consumables, for this work, ships that transport hydrogen as cargo are assumed to

consume part of the hydrogen cargo for transportation. Therefore, no proportional voyage costs are expected, but the cargo consumed during the round trip will be counted as a cost of energy loss. The non-proportional costs of the voyage, such as taxes, marine pilot and tug services, depend on the harbour and the different characteristics of the vessel.[21] A total of 15 kUSD of non-proportional voyage costs are assumed per land terminal. Insofar as loading and offloading, the facilities are included in the analysis of this logistic chain, therefore, no additional tolls or fees are foreseen.

The time of one roundtrip t_{RT} can be estimated by:

$$t_{RT} = 2 \cdot \frac{l}{s_V} + t_{LS} + \frac{V_H}{\dot{V}_L} + \frac{m_{OL}}{\rho_l(1\ \text{bar}) \cdot \dot{V}_{OL}} \quad \text{(Eq. S16)}$$

where l is the distance between ends; s_V is the speed of the vessel during cruise; t_{LS} represents the additional time during the approach and departure at both end terminals at low speed; V_H represents the volume of the holds; $\dot{V}_L$ is the loading flow rate of the liquefied hydrogen; m_{OL} represents the off-loaded mass of hydrogen at the receiving terminal; $\rho_l(1\ bar)$ represents the saturation density of liquid hydrogen at 1 bar and $\dot{V}_{OL}$ represents the off-loading flow rate of the liquefied hydrogen

The offloaded mass of hydrogen m_{OL} is calculated by:

$$m_{OL} = m_L - m_C \quad \text{(Eq. S17)}$$

where m_L is the loaded mass of hydrogen; which coincides with the total cargo capacity of the vessel and m_C is the hydrogen consumed during the roundtrip.

The consumed mass of hydrogen m_C is estimated by means of:

$$m_C = 2 \cdot \frac{l}{s_V} \cdot cr_C + \left(\frac{V_H}{\dot{V}_L} + \frac{m_{OL}}{\rho_l(1\ bar) \cdot \dot{V}_{OL}} \right) \cdot cr_{L,OL} \quad \text{(Eq. S18)}$$

Here cr_C is the consumption rate of hydrogen during navigation and $cr_{L,OL}$ is the consumption rate of hydrogen during loading and offloading.

The number of ships needed in the fleet N_{ships} can be calculated by:

$$N_{ships} = \frac{\dot{m}_{H2} \cdot t_{RT}}{m_L} \quad \text{(Eq. S19)}$$

where $\dot{m}_{H2}$ is the mass flow rate of the produced hydrogen.

If the number of ships is not an integer, then, the velocity of the ship during navigation is reduced, until Eq. **Error! Reference source not found.** yields a whole number. The reduction of the ship velocity, s_V, also reduces the consumption rate of hydrogen during cruising, cr_C, according to the cubic rule:

$$cr_C = \frac{\dot{W}_{nom}}{\eta_{FC} \cdot LHV} \cdot \left(\frac{s_V}{s_{V_{nom}}} \right)^3 \quad \text{(Eq. S20)}$$

where $\dot{W}_{nom}$ is the power developed at cruise speed; η_{FC} is the fuel cell efficiency; LHV is the Lower Heating Value of hydrogen and $s_{V_{nom}}$ the nominal cruise speed of the ship.

The number of voyages throughout the assumed operational lifetime $N_{voyages}$ can be estimated by:

$$N_{voyages} = \frac{t_L}{t_{RT}} \quad \text{(Eq. S21)}$$

where t_L is the life cycle time.

The life cycle cost of the fleet of ships C_{fleet} can be estimated by:

$$C_{fleet} = N_{ships} \cdot (t_{RT} \cdot c_{TC} + C_V) \quad \text{(Eq. S22)}$$

where c_{TC} is the time charter rate and C_V the voyage costs for one round trip.

Table S6 contains the baseline assumptions used for the thermo-economic calculations of the ships for the transportation of hydrogen.

Table S6. Assumptions for the LH2 fleet.

Parameter	Value	Uncertainty
c_{TC} (kUSD/d)	90	10%
C_V (kUSD/round trip·land terminal)	15	10%
Ship capacity (t_{H2})	12,760	5%
V_H (m^3)	180,000	5%

Nominal pressure (bar)	1	-
Min pressure (bar)	1	-
$s_{V_{nom}}$ (kn)	20	10%
$s_{V_{nom}}$ (m/s)	10.29	10%
$\dot{W}_{nom}$(sailing) (MW)[22–24]	35	5%
$\dot{W}_{nom}$ (Loading and offloading) (MW)	2	10%
Power plant efficiency η_{FC} (based on LHV_{H2})	0.55	5%
t_{LS} (s)	3,600	5%
$\dot{V}_L$ (m^3/h)	12,000	5%
$\dot{V}_{OL}$ (m^3/h)	12,000	5%

1.1.4 Hydrogen regasification plant

Some refuelling stations use evaporators to obtain hydrogen under conditions suitable for storage in vehicles. Regarding the cost model, HDSAM Version 3.0 incorporates cost data for a facility with this technology. An equation is presented in HDSAM that illustrates the relationship between the uninstalled cost of evaporators and the mass flow of hydrogen obtained. It is adjusted for annual inflation:

$$C_{Regasif} = (595293 \cdot \dot{m}_{H2} + 122) \cdot f_{install} \quad \text{(Eq. S23)}$$

where $\dot{m}_{H2}$ represent the mass of hydrogen measured in kg/s and $f_{install}$ is the installation factor.

Table S7 contains the baseline assumptions used for the thermo-economic calculations of the hydrogen regasification plant.

Table S7. Assumptions for the regasification plant.

Parameter	Value	Uncertainty
$f_{install}$	1.3	5%
M-L refurbishment ($\%C_{Regasif}$)	200%	5%
End of Life ($\%C_{Regasif}$)	5%	5%

1.2 Facilities shared between methanol alternatives

1.2.1 Methanol synthesis plant

The cost of a methanol synthesis plant has been obtained in this work as a function of the mass flow of methanol that it can produce. A regression is made based on the economic information of methanol synthesis plants published by the International Renewable Energy Agency.[25] The data includes the cost of an electrolysis plant for producing the hydrogen needed for the synthesis of methanol. Therefore, in order to obtain the cost of the synthesis facility, the cost of the

electrolysis plant estimated in this study, including refurbishment, has been deducted from the total cost obtained with the regression:

$$C_{Synth} = 57348390 \cdot \dot{m}_{MeOH}^{0.9086808} - 3 \cdot C_{EC} \quad \text{(Eq. S24)}$$

where $\dot{m}_{MeOH}$ is expressed in kg/s.

The O&M cost of a methanol synthesis plant includes fixed OPEX and the cost of CO_2 needed for this process. Fixed OPEX is obtained as a percentage of fixed capital investment.[26] CO_2 and H_2 mass flow needed for methanol production are obtained from the parameters published: 1.397 $kgCO_2/kgMeOH$, 0.192 $kgH_2/kgMeOH$.[26] Electric energy consumption is related to the mass flow of methanol produced, 0.175 MWh/t.[26]

Table S8 contains the baseline assumptions used for the thermo-economic calculations of a methanol synthesis facility.

Table S8. Assumptions for a methanol synthesis plant

Parameter	Value	Uncertainty
H_2 usage ($kgH_2/kgMeOH$)[26]	0.192	5%
CO_2 usage ($kgCO_2/kgMeOH$)[26]	1.397	5%
CO_2 cost ($/kg)[26]	0.0229	5%

M-L refurbishment (% C_{Synth})	200%	5%
Yearly Fixed O&M (% C_{Synth})[26]	1.5%	5%
End of Life (%C_{Synth})	10%	5%

1.2.2 Methanol storage facilities

The cost of methanol storage tanks in this study does not benefit from scale effects since the price of a 200 tons methanol tank is used as the basis for the cost estimation. The following equation is used to calculate the cost of the storage facility:[27]

$$C_{SMeOH} = 53.1 \cdot m_{MeOH} \quad \text{(Eq. S25)}$$

where m_{MeOH} represents the maximum storage capacity of methanol storage facilities measured in kg.

Table S9 contains the baseline assumptions used for the thermo-economic calculations of methanol tanks.

Table S9. Assumptions for methanol storage facilities

Parameter	Value	Uncertainty
M-L refurbishment (%C_{SMeOH})	100%	5%
End of Life (%C_{SMeOH})	5%	5%

1.2.3 Methanol carrier ship

Although there are ships designated for the transport of methanol today[28], not enough economic data has been found on this specific type of ship to develop a reliable model. Nevertheless, due to the similarities between ships presently transporting methanol and tanker ships, the costs of the latter can be used as a benchmark for estimating methanol freight rates. Published economic data [29] of tanker ships presents a time charter average rate of 16,918 USD/day for a LR1 (74,000 dwt) tanker ship in 2020. Taking into account annual inflation and information of a larger ship (120,000 m^3)[28] that currently transports methanol, an estimated time charter rate of 19,000 USD/day is considered in this study. Regarding consumables, for this work, ships that transport methanol as cargo are assumed to consume part of the methanol cargo for transportation. A total of 15 kUSD of non-proportional voyage costs are assumed per land terminal. As per loading and offloading, the facilities are included in the analysis of this logistic chain, therefore no additional tolls or fees are foreseen.

The model of methanol transport shares the characteristics of the previously described model, related to hydrogen transport. The difference lies in the characteristics of the ships that transport

each fuel. Table S10 contains the baseline assumptions used for the thermo-economic calculations for ships that transport methanol.

Table S10. Assumptions for a methanol fleet

Parameter	Value	Uncertainty
c_{TC} (kUSD/d)	19	10%
C_V (kUSD/round trip·land terminal)	15	10%
Ship capacity (t_{MeOH})	95,040	5%
V_{MeOH} (m^3)	120,000	5%
Nominal pressure (bar)	1	-
Min pressure (bar)	1	-
$s_{V_{nom}}$ (kn)	15.4	5%
$s_{V_{nom}}$ (m/s)	7.92	5%
$\dot{W}_{nom}$(sailing) (MW)	15	5%
$\dot{W}_{nom}$ (Loading and offloading) (MW)	2	5%
Power plant efficiency η_{engine} (based on LHV_{MeOH})	0.35	5%
t_{LS} (s)	3,600	5%
$\dot{V}_L$ (m^3/h)	12,000	5%
$\dot{V}_{OL}$ (m^3/h)	12,000	5%

1.3 Exclusive facilities of methanol alternative with electrolysis

1.3.1 Methanol electrolysis plant

Currently, there are no commercial methanol electrolysis units. However, the designs of PEM methanol electrolysis and PEM water electrolysis are similar. This fact can be used to predict the cost of the methanol electrolysis unit with reasonably low uncertainty. The models for the cost estimation of the methanol electrolyser are based on the model used for PEM water electrolysis. To adjust the model, first, all the differences between methanol and water electrolysis systems are listed, then the pertinent corrections are applied to the water PEME electrolysis unit model.

The catalyst composition and its content are different in methanol and water PEME. Methanol electrolysis cells contain platinum and ruthenium between 1.5-2.0 mg/cm^2[30]. However, PEM water electrolysis cells contain approximately 0.8 mg/cm^2 of platinum and 2.5 mg/cm^2 of iridium.[31] In the case of methanol PEME, the catalyst cost is equivalent to about $2.60 \cdot 10^{-2}$ USD/cm^2 and in the case of water PEME, the catalyst cost is equivalent to $8.29 \cdot 10^{-2}$ USD/cm^2. The catalyst-coated membrane has an impact of about 25%-45% on the cost breakdown of a commercial PEM water electrolyser.[32] In turn, the catalysts comprise between 30% to 50% of the catalyst-coated membrane.[32] This means that the impact of these precious metals ranges from 7.5%-22.5% of the total cost. Therefore, for the same area and number of cells of an electrolysis

unit, the cost factor that calculates the cost of the equivalent Methanol electrolysis cell ranges between 1.239 and 1.717.

The polarization curves of methanol electrolysers show lower current densities and lower faradaic efficiencies. Both effects mean larger electrolysis stacks for the same hydrogen production rate, which leads to costlier electrolysis stacks. While water PEM electrolysis stacks normally operate at around 1 A/cm^2,[31] the methanol equivalents would operate at much lower current densities to keep a reasonable efficiency. A good trade-off between the electrolysis rate and the efficiency could be 150 mA/cm^2, while the cell voltage is approximately 0.5 V for most reported methanol electrolysis units in the literature. This involves an electric efficiency of approximately 0.45, while having a practical current density. This effect would increase the size of the PEM equivalent 6.7 times. By assuming an electrolysis standard of 150 mA/cm^2, a factor corresponding to $j_0^{0.32} = 0.150^{0.32} = 0.5449$, is applied. The faradaic efficiencies in this range of current density range between 0.70 and 0.75.[33] This means that for the same hydrogen output, the size of the electrolysis unit increases by a factor between 1.3 and 1.4.

With this information, the extrapolated model for methanol fuel cells is:

$$C_{EC} = (663894313 \pm 131158196) \cdot \frac{\dot{m}_{H_2}{}^{0.79}}{j^{0.32}} \quad \text{(Eq. S26)}$$

where $\dot{m}_{H_2}$ is expressed in $(\mathrm{kg/s})$ and the current density j in $(\mathrm{A/cm^2})$.

The O&M routines are expected to be identical to those of a PEME electrolyser. For this reason, the expected annual O&M cost is 6 USD/kW.[9] The lifespan of an electrolyser can be up to 100,000 h.[9] Therefore, at least two complete midlife refurbishments could be expected.

The electric power consumed by the electrolysis plant $\dot{W}_{ext,meth-electrol}$ can be calculated by:

$$\dot{W}_{ext,meth-electrol} = \frac{\dot{m}_{\mathrm{H_2}} \cdot h_{\mathrm{H_2}} + \dot{m}_{\mathrm{CO_2}} \cdot h_{\mathrm{CO_2}} - \dot{m}_{\mathrm{H_2O}} \cdot h_{\mathrm{H_2O}} - \dot{m}_{\mathrm{CH_3OH}} \cdot h_{\mathrm{CH_3OH}}}{\eta_{meth-electrol}} \quad \text{(Eq. S27)}$$

where $\dot{m}_{\mathrm{H_2}} = \frac{M_{\mathrm{H_2}}}{M_{\mathrm{H_2O}}} \cdot \dot{m}_{\mathrm{H_2O}} \cdot 3$; $\dot{m}_{\mathrm{CO_2}} = M_{\mathrm{CO_2}}/M_{\mathrm{H_2O}} \cdot \dot{m}_{\mathrm{H_2O}}$; $\dot{m}_{\mathrm{CH_3OH}} = M_{\mathrm{CH_3OH}}/M_{\mathrm{H_2O}} \cdot \dot{m}_{\mathrm{H_2O}}$, and the enthalpies are obtained as:

$$h_{\mathrm{CO_2}} = \Delta h^0_{f_{\mathrm{CO_2}}}(T^0,p^0) + \left[h_{\mathrm{CO_2}}(T,p) - h_{\mathrm{CO_2}}(T^0,p^0)\right] \quad \text{(Eq. S28)}$$

$$h_{\mathrm{CH_3OH}} = \Delta h^0_{f_{\mathrm{CH_3OH}}}(T^0,p^0) + \left[h_{\mathrm{CH_3OH}}(T,p) - h_{\mathrm{CH_3OH}}(T^0,p^0)\right] \quad \text{(Eq. S29)}$$

Here, $\Delta h^0_{f_i}$ is the enthalpy of formation of the substance i at (T^0,p^0), and $\left[h_{\mathrm{i}}(T,p) - h_i(T^0,p^0)\right]$ is the enthalpy increment of the substance i from (T^0,p^0) to (T,p).

As with PEME water electrolysis, the power consumed by the electrolysis plant does not coincide with energy losses. The energy lost in the transformation of electricity into hydrogen is calculated by:

$$\left.\frac{dE}{dt}\right|_{lost} = \dot{W}_{ext,meth-electrol} - \dot{m}_{\mathrm{H_2}} \cdot HHV_{\mathrm{H_2}} \quad \text{(Eq. S30)}$$

For the calculation of the levelized cost of hydrogen, $\dot{W}_{ext,meth-electrol}$ is used. However, for the life cycle cost, $\left.\frac{dE}{dt}\right|_{lost}$ is used.

Error! Reference source not found. Table S11 contains the baseline assumptions used for the thermo-economic calculations of the electrolysis plant.

Table S11. Assumptions for the methanol electrolysis plant

Parameter	Value	Uncertainty
j (A/cm^2)	0.150	5%
$\eta_{electrol}$	0.3397	5%
Yearly O&M (%$C_{electrol}$)	0.2%	5%
M-L refurbishment (% $C_{electrol}$)	200%	5%
End of Life (%$C_{electrol}$)	10%	5%
T^0 (˚C)	25	1%
$T_{\mathrm{CO_2}}$ (˚C)	80	1%
$T_{\mathrm{H_2}}$ (˚C)	80	1%
$T_{\mathrm{H_2O}}$ (˚C)	25	1%
$T_{\mathrm{CH_3OH}}$ (˚C)	25	1%
p^0 (kPa)	100	1%

p_{O_2} (kPa)	5,000	1%
p_{H_2} (kPa)	5,000	1%
p_{H_2O} (kPa)	5,000	1%
p_{CH_3OH} (kPa)	5,000	1%
$\Delta h^0_{f_{H_2}}(T^0,p^0)$ (kJ/mol)[4]	0	0%
$\Delta h^0_{f_{CO_2}}(T^0,p^0)$ (kJ/mol)[4]	-393.522	0%
$\Delta h^0_{f_{H_2O}}(T^0,p^0)$ (kJ/mol)[4]	-285.830	0%
$\Delta h^0_{f_{CH_3OH}}(T^0,p^0)$ (kJ/mol)	-238.81	0%
HHV_{H_2} (MJ/kg)[10]	141.88	0%

1.4 Exclusive facilities of methanol alternative with reforming

1.4.1 Steam reforming plant

To carry out this study, two types of methanol steam-reforming plants have been considered: a packed bed reactor (PBR) and a membrane reactor (MR). Although both types of reactors produce CO_2 during their operation, the mass flow of carbon dioxide emitted during the hydrogen generation in an MR is lower than that of a PBR. There are various studies related to the reforming of methanol in a PBR.[34] Characteristics of this type of reactor include high operating temperatures and the need to install a pressure swing adsorption to purify the hydrogen obtained. Meanwhile, in an MR, the capacity of reforming and separating are combined, thereby

allowing operation at lower temperatures and a reduction in costs. Due to the aforementioned characteristics, this study analyses the cost of a methanol steam-reforming plant that uses an MR.

To obtain the cost of the methanol-reforming facility, a regression has been performed with the information about membrane reactors published in Byun et al.[35] In this way, an equation has been obtained that explains the relationship between the cost of the installation with the mass flow of hydrogen obtained after reforming:

$$C_{Reform} = 2128558 \cdot \dot{m}_{H_2}{}^{0.600} \quad \text{(Eq. S31)}$$

where $\dot{m}_{H_2}$ is expressed in kg/s.

To obtain O&M cost of methanol steam-reforming facility a regression is made with information published in Byun et al.[35] With this regression, an equation is obtained that relates the annual cost of facility operation with the mass flow of hydrogen produced:

$$C_{O\&M\ Reform} = 400378 \cdot \dot{m}_{H_2}{}^{0.276} \quad \text{(Eq. S32)}$$

As it is necessary to provide thermal energy to the system so that methanol can be reformed to obtain hydrogen, normally this type of installation produces natural gas consumption. In this study, it has been decided to use the combustion of the methanol that reaches the facility to obtain this contribution of thermal energy. The mass flow of methanol necessary to carry out the reforming process is obtained from the data of the efficiency of a methanol reforming reactor:

$$\dot{m}_{MeOH_{Combustion}} = \dot{m}_{MeOH}\left(1 - \frac{\frac{LHV_{MeOH}}{LHV_{H_2}} \cdot \eta_{reform}}{r_{conv}}\right) \quad \text{(Eq. S33)}$$

where $\dot{m}_{MeOH}$ represents the mass flow of methanol that arrives at the facility in kg/s, LHV represents the lower heating value of methanol and hydrogen in MJ/kg, η_{reform} represents the efficiency of methanol reforming reactor and r_{conv} represents the mass ratio of hydrogen converted to methanol in the reforming process expressed in kg_{H2}/kg_{MeOH}.

Table S12 contains the baseline assumptions used for the thermo-economic calculations of the methanol steam reforming plant.

Table S12. Assumptions for the methanol steam reforming plant

Parameter	Value	Uncertainty
η_{reform}	85%	5%
r_{conv} (kg_{H2}/kg_{MeOH})	0.189	5%
M-L refurbishment (% C_{Reform})	200%	5%
End of Life (%C_{Reform})	20%	5%

2. References

(1) Washington, D. C. I. A. The World Factbook https://www.cia.gov/the-world-factbook/ (accessed 2022-01-18).

(2) Westermann, D.; Hertem, D.; Real, G.; Rauhala, T.; Meisingset, M.; Kurrat, M.; Deppe, B.; Atmuri, R.; Kuester, A.; Soerangr, D.; Asplund, G.; Takasaki, M.; Klöckl, B.; Bennett, M.; Friedrich, K. Voltage Source Converter (VSC) HVDC for Power Transmission – Economic Aspects and Comparison with Other AC and DC Technologies. 2012.

(3) Lemmon, E. W.; Huber, M. L.; McLinden, M. O. NIST Standard Reference Database 23: Reference Fluid Thermodynamic and Transport Properties-REFPROP, Version 9.0.

(4) M.W. Chase Jr. NIST-JANAF Themochemical Tables (Journal of Physical and Chemical Reference Data Monograph No. 9); American Institute of Physics: Woodbury, New York, 1998.

(5) El-Emam, R. S.; Dincer, I. Thermodynamic and Thermoeconomic Analyses of Seawater Reverse Osmosis Desalination Plant with Energy Recovery. Energy 2014, 64, 154–163, DOI 10.1016/J.ENERGY.2013.11.037.

(6) Bejan, A.; Tsatsaronis, G. (George); Moran, M. J. Thermal Design and Optimization; Wiley, New York, 1996.

(7) Lümmen, N.; Karouach, A.; Tveitan, S. Thermo-Economic Study of Waste Heat Recovery from Condensing Steam for Hydrogen Production by PEM Electrolysis. Energy Convers. Manag. 2019, 185, 21–34, DOI 10.1016/j.enconman.2019.01.095.

(8) Oi, T.; Wada, K. Feasibility Study on Hydrogen Refueling Infrastructure for Fuel Cell Vehicles Using the Off-Peak Power in Japan. Int. J. Hydrogen Energy 2004, 29 (4), 347–354, DOI 10.1016/S0360-3199(03)00152-6.

(9) Schmidt, O.; Gambhir, A.; Staffell, I.; Hawkes, A.; Nelson, J.; Few, S. Future Cost and Performance of Water Electrolysis: An Expert Elicitation Study. Int. J. Hydrogen Energy 2017, 42 (52), 30470–30492, DOI 10.1016/J.IJHYDENE.2017.10.045.

(10) Godula-Jopek, A. Hydrogen Production by Electrolysis; John Wiley & Sons, 2015.

(11) A, E.; K, R. H2A Hydrogen Delivery Scenario Model (HDSAM) 2015:The Hydrogen Delivery Scenario Analysis Model; 2015.

(12) Aasadnia, M.; Mehrpooya, M. Large-Scale Liquid Hydrogen Production Methods and Approaches: A Review. Appl. Energy 2018, 212 (C), 57–83, DOI 10.1016/J.APENERGY.2017.12.033.

(13) Chen, T.-P. Hydrogen Delivery Infrastructure Options Analysis; 2010.

(14) The Future of Hydrogen; OECD, 2019, DOI 10.1787/1e0514c4-en.

(15) Cardella, U.; Decker, L.; Sundberg, J.; Klein, H. Process Optimization for Large-Scale Hydrogen Liquefaction. Int. J. Hydrogen Energy 2017, 42 (17), 12339–12354, DOI 10.1016/J.IJHYDENE.2017.03.167.

(16) Mazioli, F. C.; Rosa, R. de A.; Sagrilo, R. G. V.; Vitorugo, L. R.; Neves, B. dos S. Assessment of the Impact of Charter Party Clauses and Port's Characteristics on the Port's Financial Result. Comput. Ind. Eng. 2019, 128, 70–90, DOI 10.1016/J.CIE.2018.12.027.

(17) Plomaritou, E.; Papadopoulos, A. Shipbroking and Chartering Practice (Lloyd's Practical Shipping Guides); Taylor & Francis Group, 2017.

(18) World's First Liquefied Hydrogen Carrier SUISO FRONTIER Launches Building an International Hydrogen Energy Supply Chain Aimed at Carbon-free Society | Kawasaki Heavy Industries, Ltd. https://global.kawasaki.com/en/corp/newsroom/news/detail/?f=20191211_3487&wovn=es (accessed 2022-01-18).

(19) IGU. World LNG Report 2019; 2019. https://www.igu.org/resources/igu-world-lng-report-2019/ (accessed 2022-02-24).

(20) Steuer, C. Outlook for Competitive LNG Supply; 2019, DOI 10.26889/9781784671310.

(21) H. Meersman; S. P. Strandenes; E. Van de Voorde. Handbook of Research Methods and Applications in Transport Economics and Policy. In Handbook of research methods and applications in transport economics and policy; Edward Elgar Publishing, 2015; p 444.

(22) MAN. Propulsion Trends in LNG Carriers; 2013.

(23) Sinha, R. P.; Mohd Norsani Wan Nik, W. Investigation of Propulsion System for Large LNG Ships. IOP Conf. Ser. Mater. Sci. Eng. 2012, 36 (1), 012004, DOI 10.1088/1757-899X/36/1/012004.

(24) R. Faizal; M. Holmlund-Sund. Wärtsilä's energy efficient propulsion system selected by Indonesian owner for world's first ever CNG carrier https://www.wartsila.com/media/news/05-02-2015-wartsila's-energy-efficient-propulsion-system-selected-by-indonesian-owner-for-world's-first-ever-cng-carrier (accessed 2022-01-18).

(25) International Renewable Energy Agency (IRENA). Innovation Outlook: Renewable Methanol; 2021.

(26) Nyári, J.; Magdeldin, M.; Larmi, M.; Järvinen, M.; Santasalo-Aarnio, A. Techno-Economic Barriers of an Industrial-Scale Methanol CCU-Plant. J. CO2 Util. 2020, 39, 101166, DOI 10.1016/J.JCOU.2020.101166.

(27) Chen, C.; Yang, A. Power-to-Methanol: The Role of Process Flexibility in the Integration of Variable Renewable Energy into Chemical Production. Energy Convers. Manag. 2021, 228, 113673, DOI 10.1016/J.ENCONMAN.2020.113673.

(28) Wärtsilä. Methanol carrier MILLENNIUM EXPLORER https://www.wartsila.com/encyclopedia/term/methanol-carrier-millennium-explorer (accessed 2022-01-18).

(29) Clarkson Research Services Limited. Shipping Intelligence Weekly, Issue 1480. 2021.

(30) Ju, H. K.; Giddey, S.; Badwal, S. P. S.; Mulder, R. J.; Gengenbach, T. R. Methanol-Water Co-Electrolysis for Sustainable Hydrogen Production with PtRu/C-SnO2 Electro-Catalyst. Ionics (Kiel). 2018, 24 (8), 2367–2378, DOI 10.1007/S11581-017-2371-8.

(31) Carmo, M.; Keeley, G. P.; Holtz, D.; Grube, T.; Robinius, M.; Müller, M.; Stolten, D. PEM Water Electrolysis: Innovative Approaches towards Catalyst Separation, Recovery and Recycling. Int. J. Hydrogen Energy 2019, 44 (7), 3450–3455, DOI 10.1016/J.IJHYDENE.2018.12.030.

(32) Mayyas, A. T.; Ruth, M. F.; Pivovar, B. S.; Bender, G.; Wipke, K. B. Manufacturing Cost Analysis for Proton Exchange Membrane Water Electrolyzers; Golden, CO (United States), 2019, DOI 10.2172/1557965.

(33) Sethu, S. P.; Gangadharan, S.; Chan, S. H.; Stimming, U. Development of a Novel Cost Effective Methanol Electrolyzer Stack with Pt-Catalyzed Membrane. J. Power Sources 2014, 254, 161–167, DOI 10.1016/j.jpowsour.2013.12.103.

(34) Kim, S.; Yun, S. W.; Lee, B.; Heo, J.; Kim, K.; Kim, Y. T.; Lim, H. Steam Reforming of Methanol for Ultra-Pure H2 Production in a Membrane Reactor: Techno-Economic Analysis. Int. J. Hydrogen Energy 2019, 44 (4), 2330–2339, DOI 10.1016/J.IJHYDENE.2018.08.087.

(35) Byun, M.; Lee, B.; Lee, H.; Jung, S.; Ji, H.; Lim, H. Techno-Economic and Environmental Assessment of Methanol Steam Reforming for H2 Production at Various Scales. Int. J. Hydrogen Energy 2020, 45 (46), 24146–24158, DOI 10.1016/J.IJHYDENE.2020.06.097.